

X.P. HU¹
G. ZHAO¹
C. ZHANG¹
Z.D. XIE¹
J.L. HE²
S.N. ZHU^{1,✉}

High-power, blue-light generation in a dual-structure, periodically poled, stoichiometric LiTaO₃ crystal

¹ National Laboratory of Solid State Microstructures, Nanjing University, Nanjing 210093, P.R. China
² Institute of Crystal Materials, Shandong University, Jinan 250100, P.R. China

Received: 13 September 2006/

Revised version: 21 November 2006

Published online: 20 January 2007 • © Springer-Verlag 2007

ABSTRACT High-power blue light was generated from a diode-side-pumped Q-switched 1319 nm Nd:YAG laser with a periodically poled, stoichiometric LiTaO₃ (PPSLT) crystal. The PPSLT sample used in this experiment consists of two segments in series: the first segment has a period of 14.08 μm for the second harmonic generation (SHG) and the second segment has periods of around 4.6 μm for the generation of blue light by mixing fundamental and SH. An average power of 466 mW of a 440 nm blue light was obtained at the fundamental power of ~ 5.4 W with a conversion efficiency of 8.6%. The output power fluctuated by 3% over a half-hour period. This result indicates that our scheme is a practical method to construct a reliable compact blue laser.

PACS 42.70.Mp; 42.79.Nv; 42.55.Xi

1 Introduction

High power blue light is urgently desired for many applications, such as optical data storage, communications, spectroscopy, large image projection and medical applications. A diode-pumped solid state blue laser is a promising candidate for such applications due to the simplicity, high electrical to optical efficiency and long reliable operation life.

Our previous work [1] reported that 153 mW average power of blue light at 447 nm was generated from a dual-structure, periodically poled LiTaO₃ (PPLT) by frequency tripling a Nd:YVO₄ laser at 1342 nm with an optical-to-optical efficiency from 808 nm to 447 nm of 1.2%. The Nd:YVO₄ laser was end-pumped by a fiber-coupled 808 nm laser diode (LD). In this work, an LD-side-pumped Nd:YAG laser replaced an LD-end-pumped Nd:YVO₄ laser as a fundamental source, and a dual-structure, periodically poled stoichiometric LiTaO₃ (PPSLT) replaced the PPLT crystal. Although the same transition ${}^4F_{3/2} - {}^4I_{13/2}$ of Nd³⁺ ion can occur in these two hosts, Nd:YAG and Nd:YVO₄, their emission wavelengths in infrared (IR) are different, 1319 nm for Nd:YAG and 1342 nm for Nd:YVO₄. The discrepancy orig-

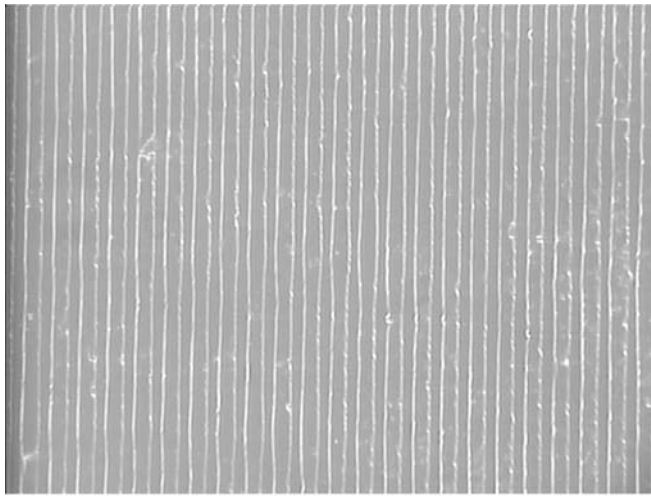
inates from the different crystal fields in two such hosts where active Nd³⁺ ions are located. By frequency tripling these two emission lines, 1319 nm and 1342 nm, blue light of 440 nm and 447 nm could be obtained, respectively. In the experiment, an LD-side-pumped approach was used. For an end-pumped geometry, a good beam profile match between the laser and the pump can be easily realized by fiber coupling. In contrast, the side-pump geometry can provide higher power or energy but a worse lasing mode. By single-pass frequency tripling the LD-side-pumped Nd:YAG laser at 1319 nm with a dual-structure PPSLT crystal, we obtained high power blue light at 440 nm. An output power of 466 mW of blue light was generated from 5.4 W of fundamental power with an efficiency of 8.6%. Our result proves that this scheme is of practical value for the construction of high-power, reliable, all-solid-state blue laser.

2 Design and fabrication of the dual-structure PPSLT sample

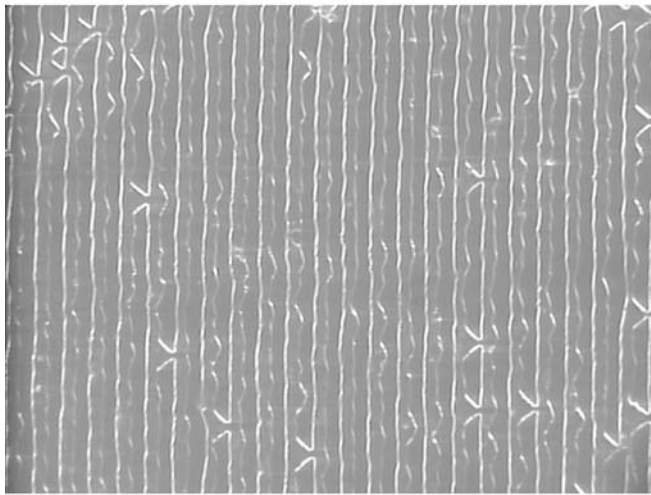
The PPSLT device used in our experiment consists of two segments in series forming a cascaded structure. The first segment was a periodic structure with the period of 14.08 μm, which carries out SHG process of 1319 nm to achieve red light at 660 nm by using its first-order quasi-phase-matched (QPM) SHG at 180 °C. Because there are some uncertainties in the coefficients of the Sellmeier equation [2] and fabrication errors of the domain pattern may arise, the second segment was designed in five parallel channels. Each channel was designed to perform the first order QPM sum-frequency generation (SFG) with the fundamental wave at 1319 nm and its second harmonic wave at 660 nm to obtain blue light at 440 nm. The channels are 1 mm wide with different periods ranging from 4.594 μm to 4.606 μm with a step of 0.003 μm. These channels ensure that phase-matching of the sum-frequency process could be accomplished by selecting a suitable channel for laser beam.

The two segments were arranged in a series and fabricated in the same stoichiometric LiTaO₃ (SLT) wafer (the SLT single wafer was purchased from Oxide Corporation) by using the conventional electrical poling technique at room temperature [3, 4]. After poling, the two end-faces of the crystal wafer were polished for optical measurement, but not coated. The wafer was 0.5 mm in thickness, and the lengths of the two seg-

✉ Fax: +86 25 83595535, E-mail: zhushn@nju.edu.cn



a



b

FIGURE 1 Structure on +Z surface of domain-inverted periods of $4.6\ \mu\text{m}$ in the PPSLT sample shown with $100\times$ magnification. (a) +Z surface, (b) -Z surface

ments were 20 mm and 10 mm, respectively. Compared with standard congruent LiTaO_3 (CLT) crystals, PPSLT exhibits high photorefractive damage resistance [5]. SLT crystals exhibits a low coercive field, one tenth that of CLT crystal [6], which allows one to pole samples with small periods. The $4.6\ \mu\text{m}$ -period for SFG was successfully fabricated, the domains revealed by etching are of high quality and the duty cycle is close to 1 : 1. This is clearly seen from Fig. 1 for both +Z and -Z surface displayed with a magnification of 100.

3 Experimental results and discussions

The experimental setup is shown in Fig. 2. The fundamental source is comprised of an LD-side-pumped Nd:YAG laser-module (RD40-1C2, CEO) that is located in a linear cavity that has the oscillating wavelength of 1319 nm. The input mirror M1 is coated with high-reflection at 1319 nm. M2 is coated to serve as an output coupler with transmission $T = 8.3\%$ at 1319 nm. Two wavelengths can be obtained around $1.3\ \mu\text{m}$ in the output of a Nd:YAG laser. One is the $R_2 - X_1$ transition at 1319 nm and the other is the $R_2 -$

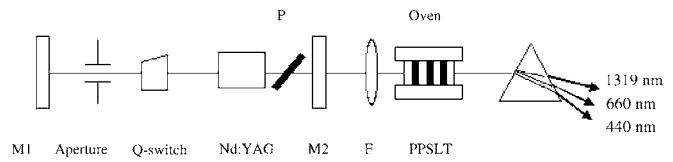


FIGURE 2 Schematic of the experimental setup

X_3 transition at 1338 nm [7]. We measured the spectrum of the fundamental wave, as displayed in Fig. 3. From the figure, we observe that, by proper design of the laser cavity, the laser operates at a single wavelength – 1319 nm and no 1338 nm line appeared in the spectrum range. An acousto-optical Q-switch in the cavity is used to change the continuous output to the pulse one with a repetition rate adjustable within the range 1–50 kHz. The pulse duration was about 160 ns at a repetition rate of 5 kHz. Because Nd:YAG is an isotropic laser medium and emits unpolarized radiation, a Brewster plate was put into the cavity in order to realize the polarized output and the polarization extinction ratio is 50 : 1. The focus length of the lens F was 100 mm, and we estimated the waist spot into the crystal to be about $300\ \mu\text{m}$. To get a high conversion efficiency of the sum frequency process, the beam waist was in the middle of the second segment of the sample. The operating current of LD was adjustable within the range 0–28 A. When the operating current was set to 28 A, we got the maximum pumping power of 600 W and the maximum fundamental output of $\sim 50\ \text{W}$, however, the beam profile of the fundamental at 1319 nm exhibited a multi-mode structure at this power level. An efficient third harmonic generation (THG) process requires a TEM_{00} fundamental mode, so an aperture was put into the cavity to select a proper TEM_{00} output. A fundamental beam with more than 5 W average power and TEM_{00} profile was obtained at the operating current of 24 A, and the M^2 of the output infrared is 1.5. The corresponding pumping power was about 470 W. When the operating current exceeded 24 A, multi-mode output would appear; thus, we set the operating current of LD to be 24 A and the repetition of Q-switch to be 5 kHz, the output power of the fundamental at 1319 nm was $\sim 5.4\ \text{W}$ and a maximum power of $\sim 466\ \text{mW}$

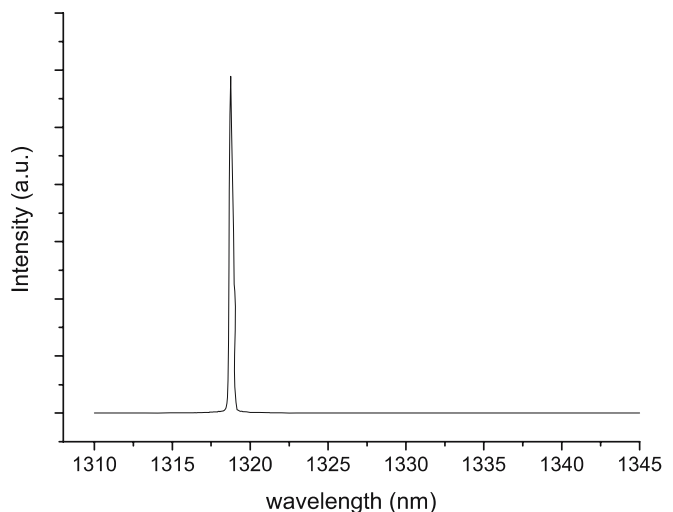


FIGURE 3 The spectrum of the fundamental wave

of blue light at 440 nm was generated from the fifth channel (in this channel, the period for SFG is 4.606 μm). The corresponding THG efficiency was 8.6% from 1319 nm to 440 nm and the overall optical-to-optical efficiency from 808 nm to 440 nm was 0.1%, much lower than that of end-pump geometry. Most of fundamental mode at 1319 nm was blocked for selection of TEM₀₀. This is a disadvantage for the side-pump geometry. In this experiment, an oven was used to heat the sample for phase-matching with an accuracy of 0.1 $^{\circ}\text{C}$. The generated red, blue and the fundamental beam were separated with a prism, and they were detected with a power meter, respectively.

Figure 4a shows the theoretical temperature tuning curves of SHG and SFG when the two processes both phase-matched at 184.0 $^{\circ}\text{C}$. Figure 4b shows the experiment results of SHG and THG output powers as a function of temperature, the theoretical curves with different phase matching temperatures of the two processes are shown as well. The measured phase-matching temperatures for SHG and THG are 184 $^{\circ}\text{C}$ and 182.6 $^{\circ}\text{C}$, with the full width at half maximum (FWHM) of 3.3 $^{\circ}\text{C}$ and 1.6 $^{\circ}\text{C}$, respectively. The measured FWHM of SFG is close to the theoretical value of 1.2 $^{\circ}\text{C}$, which indicates that the SFG is phase-matched over the whole length in the second segment. The FWHM of SHG is wider than the theoretical value of 2.0 $^{\circ}\text{C}$, a possible reason for this widening maybe the decrease of the effective length such as missing domains or unpoled regions. For the two-step scheme to realize THG, the second-harmonic process occurs in the first segment and subsequently the generated SH wave and the rest of the fundamental waves are frequency summed in the second segment to generate the TH wave. When the temperature is tuned towards the phase-matching temperature of the sum-frequency process or the output power of blue light increases, more red light is consumed in the sum-frequency process and this leads to a power reduction of the red light at output. This is clearly seen from Fig. 4. One can find that the blue light can be further increased by increasing either the fundamental power or the interaction length of SFG. In fact, there is an optimized ratio of two segments at which the maximum conversion efficiency

of blue light can be realized at a given fundamental power. We can also see from the figure that there is only a 1.4 $^{\circ}\text{C}$ temperature-shift between the two tuning curves in the fifth channel, which indicates that the multi-channel method can compensate for design errors; thus, a good phase-matching of the sum-frequency process could be obtained. At the same time, blue light generated from other channels were rather lower than from the fifth channel due to the larger phase mismatching at the measurement temperature.

Figure 5 depicts the dependence of the average output power of blue light on the incident fundamental power at 182.6 $^{\circ}\text{C}$. The THG conversion efficiency is defined as $\eta = P_t/P_f$, where P_t is the average power of 440 nm blue light, and P_f is the average power of the fundamental wave at 1319 nm. The THG conversion efficiency is $\sim 8.6\%$ at the maximum blue output, which is rather lower than the theoretical value of 18% obtained by numerical calculation of the depleted coupling wave equations. The main reason causes the reduction of the conversion efficiency is the deviation of the phase matching temperatures of SHG and SFG, and this temperature shift leads to less photons of 660 nm to participate in

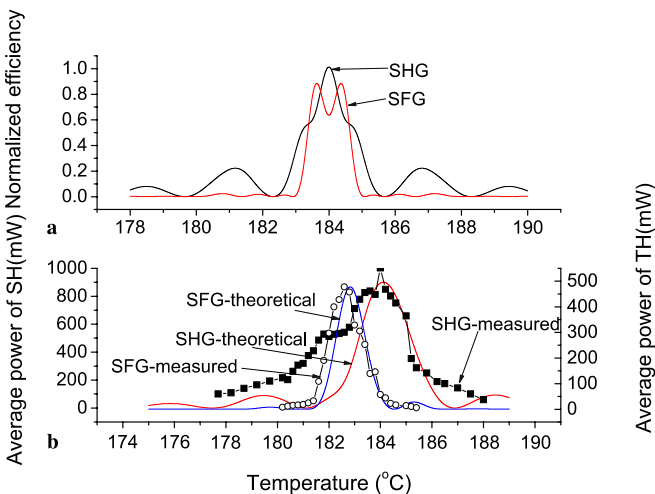


FIGURE 4 (a) Theoretical temperature tuning curves of SHG and SFG when they both phase-matched at 184.0 $^{\circ}\text{C}$; (b) measured temperature tuning curves for SHG and SFG and their theoretical curves

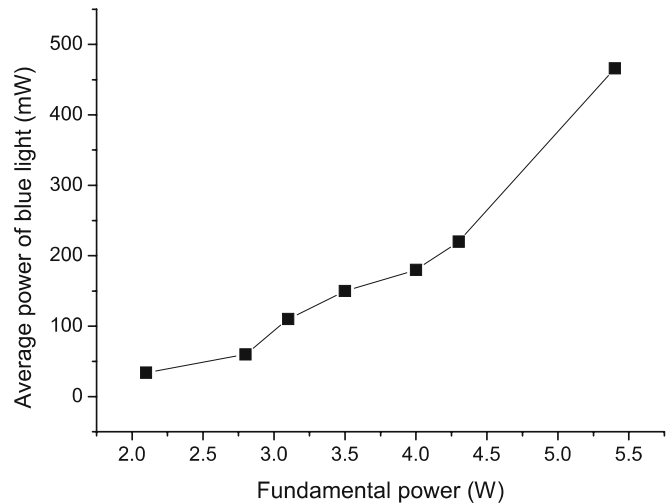


FIGURE 5 Dependence of the average output power of blue light on the incident fundamental power at 182.6 $^{\circ}\text{C}$

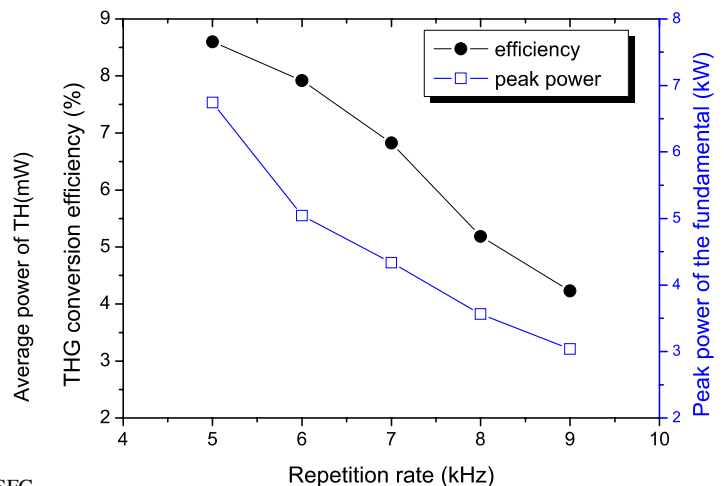


FIGURE 6 THG conversion efficiency and peak power of the fundamental wave versus the repetition rate

SFG process. As is well-known, the conversion efficiency is proportional to the peak power density $I = \frac{p}{(f\tau)A}$, where p is the average fundamental power injected into the crystal, f is the repetition rate, τ is the pulse duration and A is the fundamental beam cross area. We measured the dependence of the pulse duration on different repetition rates and found that the highest peak power and the maximum conversion efficiency took place at the repetition rate of 5 kHz, as shown in Fig. 6. At the maximum average output of 466 mW, the M^2 value was measured to be ~ 2.5 in both transverse directions. The fluctuation of power of blue light at its peak was $\sim 3\%$ during a half-hour period. According to our observation, the main factor that causes the fluctuation is the fluctuation of the fundamental wave, which is about 1%. No obvious degradation of the output power or beam quality is observed during the period, indicating that photorefractive effect is negligible at the temperature and power level.

4 Conclusion

In summary, we have realized the generation of blue light at 440 nm by frequency tripling an LD-side-pumped Q-switched Nd:YAG laser at 1, 319 nm with a dual-structure PPSLT crystal. The output of blue light at 466 mW was

achieved with the THG conversion efficiency of 8.6% when the fundamental power was 5.4 W with a repetition rate of 5 kHz. The PPSLT crystal exhibited excellent beam quality, stable output performance. No photorefractive effect was observed at the power level, indicating that PPSLT is a practical nonlinear crystal for blue laser applications.

ACKNOWLEDGEMENTS This work is supported by grants of the State Key Program for Basic Research of China (2004CB619003) and the National Natural Science Foundation of China under Contract No. 10534020 and 60578034.

REFERENCES

- 1 J.L. He, X.P. Hu, S.N. Zhu, Y.Y. Zhu, N.B. Min, *Chin. Phys. Lett.* **20**, 2175 (2003)
- 2 A. Bruner, D. Eger, M.B. Oron, P. Blau, M. Katz, S. Ruschin, *Opt. Lett.* **28**, 194 (2003)
- 3 S.N. Zhu, Y.Y. Zhu, Z.Y. Zhang, H. Shu, H.F. Wang, J.F. Hong, C.G. Ge, N.B. Ming, *J. Appl. Phys.* **77**, 5481 (1995)
- 4 V.Y. Shur, E.L. Romyontsev, E.V. Nikolaeva, E.I. Shishkin, D.V. Fursov, R.C. Batchko, L.A. Eyres, M.M. Fejer, R.L. Byer, *Appl. Phys. Lett.* **76**, 143 (2000)
- 5 K. Kitamura, Y. Furukawa, S. Takekawa, T. Hatanaka, H. Ito, V. Gopalan, *Ferroelectrics* **257**, 235 (2001)
- 6 K. Kitamura, Y. Furukawa, K. Niwa, V. Gopalan, T.E. Mitchell, *Appl. Phys. Lett.* **73**, 3073 (1998)
- 7 Y. Inoue, S. Konno, T. Kojima, S. Fujikawa, *IEEE J. Quantum Electron.* **QE-35**, 1737 (1999)